

Metabolic disposition and excretion of quinocetone in rats, pigs, broilers, and carp



Juan Li^a, Lingli Huang^a, Xu Wang^a, Yuanhu Pan^a, Zhaoying Liu^b, Dongmei Chen^a, Yanfei Tao^a, Qinghua Wu^{a,c}, Zonghui Yuan^{a,*}

^a National Reference Laboratory of Veterinary Drug Residues (HZAU)/MAO Key Laboratory for the Detection of Veterinary Drug Residues in Foods, Huazhong Agricultural University, Wuhan, Hubei 430070, China

^b Hunan Agricultural University, Veterinary Faculty, Changsha, Hunan 410128, China

^c Center for Basic and Applied Research, Faculty of Informatics and Management, University of Hradec Kralove, Hradec Kralove, Czech Republic

ARTICLE INFO

Article history:

Received 16 January 2014

Accepted 2 April 2014

Available online 12 April 2014

Keywords:

Quinocetone

Radioactivity isotope tracing

Disposition

Metabolism

Excretion

Toxicology

ABSTRACT

Excretion, disposition, and metabolism of [³H]-quinocetone in rats, pigs, broilers, and carp following oral administration were investigated. After a single p.o. dose, total radioactivity was rapidly excreted, with ≥94% in all species within 14 days. Fecal excretion of radioactivity was 68% and 65% of the administered dose in rats and pigs, respectively, with the remainder excreted in the urine. Six hours after the last of seven daily oral administrations of ³H-labeled QCT, radioactivity was found to be distributed throughout all tissues, with the majority of radioactivity cleared within 7 days, and elimination was the slowest from the liver and kidney. QCT was extensively metabolized in all of the species, and the primary changes included N–O group reduction, carbonyl group reduction, double bond reduction, and hydroxylation. The major tissue metabolites of QCT were Q2, Q4, Q5, Q8, and Q9 in rats; Q1, Q2, Q3, Q4, and Q5 in pigs; Q1, Q2, Q3, Q4, and Q7 in broilers; and Q1, Q2 in carp. This confirmed the potential link between QCT metabolism through N–O group reduction and its organ toxicity. The results of the present study provide important data that could help understand the relationship between the toxicities and metabolic disposition of QCT.

© 2014 Elsevier Ltd. All rights reserved.

1. Introduction

Quinocetone (QCT; Fig. 1), 3-methyl-2-quinoxalinbenzenevinylketo-1,4-dioxide, an antimicrobial agent, was approved by Ministry of Agriculture, PR China in 2003. It is extensively used

as a feed additive for preventing bacterial infections caused by *Salmonella*, *Escherichia coli*, *Brachyspira hyodysenteriae* and other gram-negative bacteria, and for promoting growth and feed conversion. Nevertheless, recently conducted studies have identified the adverse effects of QCT both *in vitro* and *in vivo*, such as genotoxicity, hepatotoxicity and nephrotoxicity (Ihsan et al., 2013; W. Yang et al., 2013; X. Wang et al., 2012, 2010; D. Wang et al., 2011, 2012; Yu et al., 2013). Drug metabolism and disposition generally regulates the pharmacodynamic, toxicological, and pharmacological effects of many drugs significantly, in terms of food-producing animals, metabolism also defines the residue profile of both parent drugs and metabolites in edible tissues (Antonovic and Martinez, 2011), thus determining the quality of such food animals, a major concern for the human health safety. Moreover, previous studies showed that the quinoxalines, such as carbadox (CBX) and olaquinox (OLA) were converted to several metabolites that were closely associated with their toxicities (Chen et al., 2009; FAO/WHO, 1995, 1990), particularly with the production of reduced metabolites (Beutin et al., 1981). Because QCT shares considerable structural similarity with CBX and OLA, QCT was proposed to be metabolized

Abbreviations: QCT (Q0), quinocetone; Q1, 1-desoxyquinocetone; Q2, dideoxyquinocetone; Q3, carbonyl-reduced metabolites of 1-desoxyquinocetone; Q4, carbonyl- and double-bond-reduced metabolites of 1-desoxyquinocetone; Q5, carbonyl-reduced metabolites of dideoxyquinocetone; Q6, phenyl ring hydroxylation metabolites of carbonyl-reduced quinocetone; Q7, carbonyl-reduced quinocetone; Q8, double-bond-reduced metabolite of 4-desoxyquinocetone; Q9, phenyl ring hydroxylation metabolites of quinocetone; OLA, olaquinox; CBX, carbadox; QdNOs, quinoxaline 1,4-dioxides; MQCA, 3-methylquinoxaline-2-carboxylic acid; MEQ, mequinox; QCA, quinoxaline-2-carboxylic acid; CYA, cyadox; JECFA, Joint FAO/WHO Expert Committee on Food Additives; VICH, International Cooperation on Harmonization of Technical Requirements for the Registration of Veterinary Medicinal Products; LSC, liquid scintillation counting; EIC, extracted ion chromatograms; CYP, cytochrome P450 enzyme; CBR, carbonyl reductase; H₂O₂, hydrogen peroxide; ROS, reactive oxygen species.

* Corresponding author. Tel.: +86 27 87287186; fax: +86 27 87672232.

E-mail address: yuan5802@mail.hzau.edu.cn (Z. Yuan).

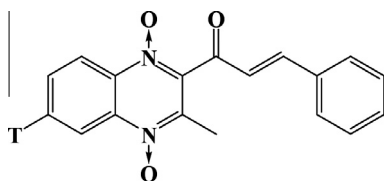


Fig. 1. Chemical structure of [^3H]-QCT.

by the same biochemical pathways as those for these drugs. 1,4-Bisdesoxyquinocetone was less toxic to liver cells than QCT (Zhang et al., 2012). QCT toxicities are apparently dependent on its metabolic pathway; however few studies were conducted on QCT disposition in laboratory animal (e.g., rats) and in food animals (e.g., pigs, broilers, and carp).

Studies have previously been conducted to examine the residual depletion of QCT in pigs, chickens, and carp, in which liver was the target tissue, 3-methylquinoxaline-2-carboxylic acid (MQCA) (Hu et al., 2008) or 3-methyl-styrylketone-quinoxaline (Zhong et al., 2012) was the marker residue, the withdrawal time of QCT was recommended as 0 days (Li et al., 2008). However, these previous studies primarily focused on QCT and a few of its known metabolites. *In vitro* and *in vivo* QCT metabolism was reported recently. A previous study showed QCT metabolism in the liver microsomes of rats by LC/MS-IT-TOF, and identified 27 metabolites (Liu et al., 2010a). *In vivo* QCT metabolism in pigs was investigated by UPLC/Q-TOF-MS, and 42 metabolites were found (Wu et al., 2012). However, tissue metabolites and quantitative analysis of the metabolite profiles were not reported.

Therefore, there is an immediate need to gain a complete understanding of the metabolic pathways, disposition kinetics, and excretion characteristic of QCT to assess the potential toxicities and food safety of this compound. According to the recommendation by JECFA, we conducted isotopic tracing studies following the guidelines of VICH (2010). We here undertook a comparative study (both quantitative and qualitative) of the metabolite profiles of QCT in rats, pigs, broilers, and carp following oral administration. Moreover, we reported the rates and routes of excretion of radioactivity of [^3H]-QCT in the urine, and feces (the mass balance for excretion). In addition, we presented QCT distribution in tissues after repeated intragastric administration of [^3H]-QCT. The present study makes contribution to improve our understanding of the food safety and the relationship between the toxicities and metabolic disposition of QCT.

2. Materials and methods

2.1. Chemicals

4- ^3H -o-nitroaniline (116 mCi/mg) was synthesized by the Shanghai Institute of Applied Physics, Chinese Academy of Sciences. QCT (99.8%) was purchased from China Institute of Veterinary Drug Control (Beijing, China). Four putative metabolites, Q1, Q2, Q3, and Q5 were synthesized at the Institute of Veterinary Pharmaceuticals (Wuhan, China), with the chemical purity of 98%. Solvable™ (tissue-solubilizing fluid), Ultima Gold and monophase A (Liquid scintillation cocktails) were purchased from PerkinElmer Life and Analytical Sciences (Groningen, The Netherlands; Waltham, MA, USA). Stop Flow™ AD scintillation liquid was obtained from the AIM Research Co. (Hockessin, DE, USA).

To a cooled stirring solution of 4- ^3H -o-nitroaniline (40 mg) and solid sodium hydroxide (16 mg) in isopropanol (240 μL), sodium hypochlorite solution (600 μL , containing 5% available chlorine) was added dropwise. The mixture was stirred at 20 °C for 4 h and filtrated to give 4- ^3H -benzofurazan-1-oxide (Xmg). After it was dissolved in methanol (100 μL), acetylacetone (150 μL) and triethylamine (400 μL) were added. The solution was then stirred for 15 h at r.t. to obtain 6- ^3H -3-methyl-2-acetyl-N-1,4-dioxyquinoxaline, which was applied to a aldol condensation reaction with benzaldehyde to give the desired products: [^3H]-QCT (Fig. 1). The final labeled product was reconstituted in ethanol to provide

210 mCi [^3H]-QCT (yield, 21%), with a radiochemical purity of 99%. Specific activity was 42 mCi/mg, and the specific activities were diluted to 11.25 mCi/g for the animal study. Exchange of the ^3H label with water was confirmed.

2.2. Animals

Male and female specific pathogen-free Wistar rats (*Rattus norvegicus*, 7 weeks, 200 \pm 10 g), were procured from the Center of Laboratory Animals of Hubei Province (Wuhan, PR China). Healthy castrated crossbred (Duroc \times Large white \times Landrace) pigs (45 days, 15 \pm 1 kg) were purchased from the Livestock and Poultry Breeding Center of Hubei Province (Wuhan, PR China). Healthy Cobb 500 broilers (28 days, 1.0 \pm 0.1 kg) were purchased from the Charoen Pokphand Group (Wuhan, PR China), and healthy carp (500 \pm 100 g) were purchased from the Wuhan Fish Breeding Farm (Wuhan, PR China). The animals and fish were maintained under standard environmental conditions using the routine methods of animal husbandry and aquaculture. Throughout the study period, feed was withheld from approximately 12 h before until 4 h after drug administration, while water was available *ad libitum*. The animals were housed singly in all-steel metabolism cages specifically designed for the separate, quantitative collection of urine and feces in a temperature-controlled room (20 \pm 2 °C) with a 12-h light/dark cycle. The Ethical Committee of the Faculty of Veterinary Medicine (Huazhong Agriculture University) approved the present study. All in-life experiments complied with the policy on the care and use of laboratory animals.

2.3. Clinical study design

2.3.1. Excretion and metabolism of [^3H]-QCT

Three male and three female rats (four pigs, six broilers, and six carp) were administered a single oral dose of [^3H]-QCT (11.25 mCi/g) by gavage at 4 mg \pm 0.4 mg (120 mg \pm 8 mg, 20 mg \pm 2 mg, and 2.5 mg \pm 0.5 mg, respectively, for the other animals) equivalent of 200 mg/kg diet. Urine and feces samples were collected into preweighed dry ice-cooled containers protected from light prior to dose administration; at intervals of 0–6 h, 6–12 h, and 12–24 h after dose administration; and then daily until two consecutive samples from urine and feces had <1% of the total administered radioactivity. The cage washings were retained with the excreta. Fourteen days after dose administration, all animals were anesthetized and killed, and pigs were slaughtered using a captive bolt stunning equipment and exsanguinated on the basis of guidelines provided by the American Veterinary Medical Association for euthanasia (AVMA, 2001). Samples were stored at -80 °C prior to analysis.

2.3.2. Distribution of [^3H]-QCT

Each of the 36 rats (20 pigs, 36 broilers, and 36 carp) were given 2 mg \pm 0.2 mg (60 mg \pm 4 mg, 10 mg \pm 1 mg, and 1.25 mg \pm 0.25 mg, respectively, for the other models) [^3H]-QCT (11.25 mCi/g) equivalent of 100 mg/kg diet by oral gavage for 7 consecutive days. At different time points [6 h, 2, 5, 9, 14, and 21 days (6 h, 1, 3, 7 and 14 days for the other animals)], six rats (four pigs, six broilers, and six carp) were anesthetized and killed, and pigs were slaughtered as described in Section 2.3.1. Blood, bile, organs and tissues (gastrointestinal tract, kidneys, liver, heart, spleen, lung, muscle, fat, skin, brain, gonad, adrenal gland, and bladder) were sampled. Samples were immediately frozen at -80 °C.

2.4. Analysis of total radioactivity

Duplicate samples were analyzed by liquid scintillation counting (LSC) until a statistical error (2σ) of 0.5% was obtained, with a counting time of 5 min, together with representative blank samples. LSC was performed using a Packard Tri-Carb 2900 liquid scintillation analyzer with automatic quench correction by an external method (PerkinElmer Life and Analytical Sciences, Waltham, MA, USA) to detect retained ^3H radioactivity. To calculate the content of volatile radioactivity such as ^3H water, another duplicate set of samples was freeze-dried and reconstituted in water ("dry samples") prior to analysis. 200 μL of the urine samples were diluted in 10 mL monophase A and subjected to LSC analysis. Feces samples were homogenized with a mixer (Omni International, USA) in equal amount of methanol/water (50/50, v/v). Subsequently, 200 mg of the homogenized samples were incubated overnight at 55 °C with 2 mL of sodium hypochlorite and subjected to LSC analysis. Before LSC analysis, whole blood (200 μL) and organ (200 mg) samples were incubated overnight at 55 °C with 2 mL of Solvable™. After incubation, the samples were decolorized with 200 μL of 0.1 mol/L EDTA-Na and 200 μL of hydrogen peroxide (30%) (500 μL in case of spleen) and counted. The efficiency of digestion was confirmed by digestion of radiochemical standards (^3H -Spec-Chec; PerkinElmer Life and Analytical Sciences, Waltham, MA, USA) for every 10–15 samples and was between 96% and 98%. A correction factor was used accordingly. All samples were prepared in 10 mL scintillation fluid (Ultima Gold) and incubated at room temperature overnight in a dark environment prior to LSC analysis.

2.5. Analysis of metabolite profiles in plasma, tissue, urine, feces, and bile

2.5.1. Urine preparation

The weight of each aliquot was 0.25% of the total fraction weight. Each urine sample was centrifuged at 4 °C for 5 min at 4000 r/min. The supernatant was collected, dried under nitrogen gas, reconstituted in 20% ACN, and further subjected to HPLC radiochemical detection.

2.5.2. Preparation of plasma, tissue, feces, and bile

The weight of each aliquot was 0.1% of the total fraction weight. Each sample was mixed two times with acetonitrile (3 mL/g of homogenate), sonicated for 5 min, and centrifuged at 4 °C for 10 min at 4000 r/min. The liquid fraction was collected, and the pellet was extracted two times with ethyl acetate (3 mL/g of homogenate), sonicated, and centrifuged. All liquid fractions collected were pooled, dried under nitrogen gas, and reconstituted in 20% ACN. The mixture was analyzed by HPLC and using the vARC™ 2.0 Radio-LC assay system Detector RS232 (AIM research co.).

2.5.3. Metabolite profiling

HPLC was performed using a 5 µm, 150 × 2.1 mm Hypersil GOLD column (Thermo Scientific Inc., USA) at a flow rate of 0.2 mL/min at 40 °C. The liquid chromatography system (Shimadzu) was equipped with a solvent delivery pump (LC-20AD), an autosampler (SIL-20AC), a DGU-20A3 degasser, a photodiode array detector (SPD-M20A), a communication base module (CBM-20A), and a column oven (CTO-20AC). The injection volume was 20 µL. The mobile phase was a binary mixture of 0.1% trifluoroacetic acid in water (solvent A) and acetonitrile (solvent B). The following gradient was used: 0–16 min, a linear gradient from 5% B to 20% B; 16–25 min, a linear gradient to 35% B; 25–30 min, a linear gradient to 60% B; 30–35 min, a linear gradient to 100% B; 35–37 min, 100% B; and 37–37.1 min, a linear gradient back to 5% B. The analysis was completed in 45 min. HPLC radiochemical detection was performed using the vARC™ 2.0 Radio-LC system Detector RS232 equipped with a 750-µL detector cell. The instrument was operated in the dynamic liquid scintillation flow mode, and the HPLC eluent was mixed 1:5 with Stop Flow™ AD scintillation liquid. After radiochemical detection, the total effluent from the detector was transferred directly to the hybrid IT/TOF mass spectrometer without splitting. Metabolites were isolated and identified as described by Liu et al. (2010a) using a Shimadzu LC/MS-IT-TOF hybrid mass spectrometer (Kyoto, Japan), which was equipped with an electrospray ionization source and operated in a positive and/or negative mode.

2.6. Data analysis

All the samples were quantitatively profiled using reversed-phase HPLC with radiochemical detection. The linear relationship between the cpm (X), which obtained from the vARC™ detector, and the dpm (Y) from Tri-Carb 2900TR was $Y = 4.24X + 1748$ ($r = 0.9990$).

3. Results

3.1. Radioactivity excretion

Following administration of a single oral dose of [³H]-QCT to rats, pigs, broilers, and carp, radioactivity excreted in the urine and feces over 0 days to 14 days after administration was 25.9% and 67.9% of the dose in female rats, 27.8% and 68.0% of the dose in male rats, and 27.2% and 65.0% of the dose in pigs, respectively.

Table 1

Excretion of radioactivity during 14 days after single oral doses of [³H]quinocetone solution (mixed with a 0.5% solution of carboxymethyl cellulose in water) to male rats ($n = 3$), female rats ($n = 3$), pigs ($n = 4$), broilers ($n = 6$), and carp ($n = 6$). Results are expressed as percentage of total radioactive dose and represent the mean of three to six animals.

Time (d)	Rat (%)				Pig (%)		Broiler (%)	Carp (%)
	Female		Male		Urine	Feces	Feces	Excreta
	Urine	Feces	Urine	Feces				
0–0.5	9.0 ± 1.2	34.6 ± 3.2	10.9 ± 1.8	37.5 ± 3.6	0.9 ± 0.1	7.3 ± 1.4	39.4 ± 3.2	18.2 ± 4.1
0.5–1	5.4 ± 0.4	24.4 ± 3.2	5.77 ± 0.6	23.1 ± 2.5	5.5 ± 0.5	17.2 ± 1.9	18.9 ± 4.1	15.6 ± 3.2
1–3	6.9 ± 0.2	5.9 ± 0.9	6.6 ± 0.4	4.9 ± 0.6	17.7 ± 0.6	29.4 ± 2.2	24.6 ± 4.1	51.3 ± 5.7
3–7	3.9 ± 0.3	1.7 ± 0.5	3.7 ± 0.5	1.4 ± 0.4	2.4 ± 0.5	9.7 ± 1.1	6.8 ± 1.5	9.1 ± 3.4
7–14	0.7 ± 0.2	1.3 ± 0.4	0.8 ± 0.1	1.1 ± 0.6	0.7 ± 0.1	1.4 ± 0.2	2.4 ± 0.7	– ^a
Sum	25.9 ± 1.5	67.9 ± 3.1	27.8 ± 3.1	68.0 ± 7.2	27.2 ± 0.4	65.0 ± 0.8	92.1 ± 1.4	94.2 ± 8.7
Cage washings	0.7 ± 0.1	0.6 ± 0.1	0.7 ± 0.1	0.8 ± 0.2	–	–	–	–
Carcass	3.7 ± 1.4	2.4 ± 0.4	5.6 ± 0.6	6.0 ± 1.1	2.6 ± 0.3	–	–	–
Total recovery	98.2 ± 2.4	98.8 ± 7.4	98.5 ± 1.2	98.9 ± 0.9	96.8 ± 7.9	–	–	–

^a Not determined.

The mean cumulative recovery of excretion, including that in cage washings within 14 days, ranged from 90% to 97%. Drug-related material was excreted rapidly, with 75% of the administered dose recovered by 24 h in both genders of rats, with 78%, 83%, and 85% of the administered dose recovered by 72 h in pigs, broilers and carp, respectively, and >96% of total radioactivity, including that in carcass, recovered within 14 days (Table 1).

3.2. Tissue distribution of [³H]-QCT (metabolites)

After [³H]-QCT was administered by gavage to rats, pigs, broilers, and carp at the daily dose of 100 mg/kg feed for 7 consecutive days, radioactivity was found in all the tissues of the analyzed animals 6 h after dose administration (Fig. 2). High radioactivity levels were detected in the liver, kidney, gastrointestinal tract, blood, bile, chicken crop, fish gill, and skin, whereas low levels were detected in the heart, spleen, lung, muscle, fat, skin, bladder, adrenal glands, and blood. In rats, although the levels declined subsequently, they were all still measurable at 48 h, with the greatest value found in the liver and kidney. Radioactivity in all of the analyzed organs and tissues declined rapidly 5 days after dose administration. Apart from the liver, kidney, bladder, and blood that had detectable levels of radioactivity, trace amount of radioactivity was observed in the other organs or tissues 9 days after dose administration. Heart, liver, spleen, lung, kidney, skin, bladder, and blood had detectable levels even 14 days after dose administration. By 21 days after dose administration, radioactivity was undetectable in any of the analyzed organs or tissues (Fig. 2A). In pigs, broilers, and carp, by 3 days, radioactivity declined to <200 µg/kg in most tissues except the liver, kidney, and small intestine, and by 7 days, radioactivity was detectable only in the liver, kidney, bile, and small intestine. However, by 14 days, no radioactivity was detected in any of the tissues examined (Fig. 2B–D).

3.3. Metabolite profiles

The extraction recovery of radioactivity from all samples was ≥90%. ³H water was not detected because of the freeze-drying step in sample preparation.

3.3.1. Rats

The results of HPLC-vARC analysis of rat plasma, systemic tissues, and excreta revealed that intact QCT was present in many samples. On the radiochromatograms, only one major metabolite peak was detected in plasma 6 h after dose administration, namely, Q5 (Fig. 3A), with the retention time corresponding to that of 3-methyl-2-phenylethylalcohol-quinoxaline. The proportion of this component declined over time and vanished at 24 h. In the

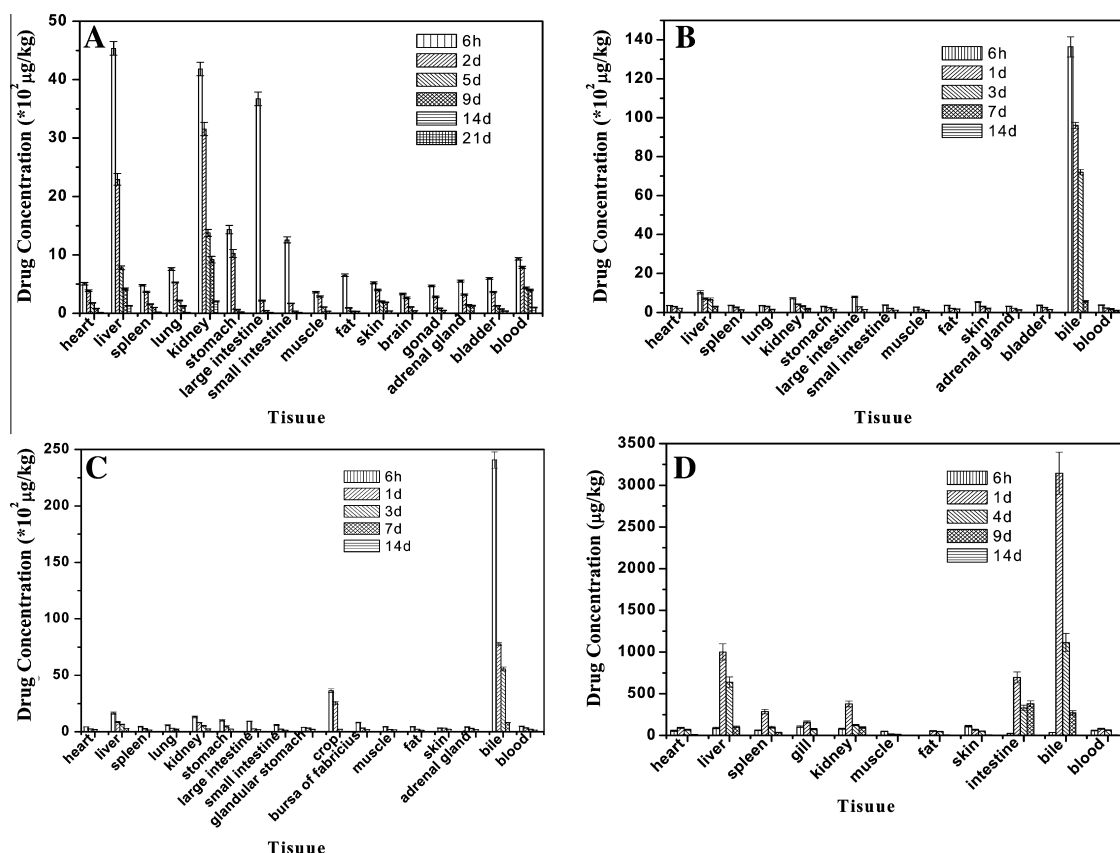


Fig. 2. Organ distribution of QCT in rats (A), pigs (B), broilers (C) and carp (D). Data show the drug concentration ($\times 10^2 \mu\text{g/kg}$) levels of $[^3\text{H}]$ -QCT (metabolites) at different time point after the last of 7 daily oral administration to animals. Values are expressed as averages \pm S.D.

examined tissue extracts, Q5 was the major radioactive metabolite in the liver and kidney 6 h after dose administration and was one of the five major metabolites in the liver and kidney 48 h after dose administration (Table 2). Another major metabolite detected in the liver and kidney 48 h after dose administration was Q8, with the proportions of 10.7% and 7.3%, respectively. Four other peaks were observed, the retention times of which corresponded to those of Q0, Q2, Q4, and Q9 on the radiochromatograms. These peaks demonstrated 8.5%, 5.6%, 10.4%, and 9.6% of liver radioactivity and 2.9%, 6.7%, 6.4%, and 5.6% of kidney radioactivity, respectively (Fig. 3B and C). On the other hand, Q8 was essentially absent from the feces, although it was present in the liver, kidney, and urine. Intact QCT was detected in the 0–12 h urine of the dosed rats as well as in the 0–12 h feces, where it displayed 69.8% and 62.8% of sample radioactivity, respectively (Fig. 3D and E). In the 0–12 h urine, the predominant metabolite, the retention time of which corresponded to that of Q9 on the radiochromatograms, displayed 19.7% of sample radioactivity. Another major peak, the retention time of which corresponded to that of Q8 on the radiochromatograms, displayed 13.5% of sample radioactivity (Fig. 3D). In the 0–12 h feces, the predominant metabolite, the retention time of which corresponded to that of Q9 on the radiochromatograms, displayed 30.8% of sample radioactivity. A minor peak, the retention time of which corresponded to that of Q4 on the radiochromatograms, displayed 2.8% of sample radioactivity (Fig. 3E).

3.3.2. Pigs

Intact QCT was detected in the 0–12 h urine and feces of the pigs administered a single dose, where it displayed 25.7% and 49.1% of sample radioactivity, respectively (Fig. 4A and B). Another predominant metabolite observed in the 0–12 h urine, the

retention time of which corresponded to that of Q2 on the radiochromatograms, displayed 61.8% of sample radioactivity. Two other minor peaks, the retention times of which corresponded to those of Q4 and Q1 on the radiochromatograms, displayed 5.1% and 3.4% of sample radioactivity, respectively. Q2 was another major metabolite in the 0–12 h feces, and it displayed 40.7% of sample radioactivity. Q1 was also observed on the radiochromatograms, and it displayed 2.8% sample radioactivity. Intact QCT and six metabolite peaks were detected in bile 6 h after dose administration on extracted ion chromatograph (EIC) (Fig. 5A). Q0, Q1, Q2, and Q5 were the major metabolites and displayed 41.1%, 15.8%, 12.0%, and 10.3% of sample radioactivity, respectively. Q3, Q4, and Q6 displayed 5.8%, 7.0%, and 8.0% of sample radioactivity, respectively.

3.3.3. Broilers

In the 0–24 h excreta of the broilers administered a single dose, Q0 was the predominant metabolite, and displayed 70.8% sample radioactivity. Two major metabolites, the retention times of which corresponded to those of Q1 and Q2 on the radiochromatograms, displayed 11.3% and 10.0% of sample radioactivity, respectively. Q4 and Q7 were also observed on the radiochromatograms and displayed 3.6% and 4.4% of sample radioactivity, respectively (Fig. 5B).

3.3.4. Carp

The metabolites observed in the 0–48 h excreta of the carp administered a single dose mirrored those observed in the 0–12 h feces of pigs, which were Q0, Q2, and Q1 that displayed 61.8%, 10.5%, and 20.9% of sample radioactivity, respectively (Fig. 5C).

Tables 2 and 3 summarize the metabolite abundance (expressed as concentration) in different matrices across the species. The major metabolites of QCT were Q2, Q4, Q5, Q8, and Q9 in rats;

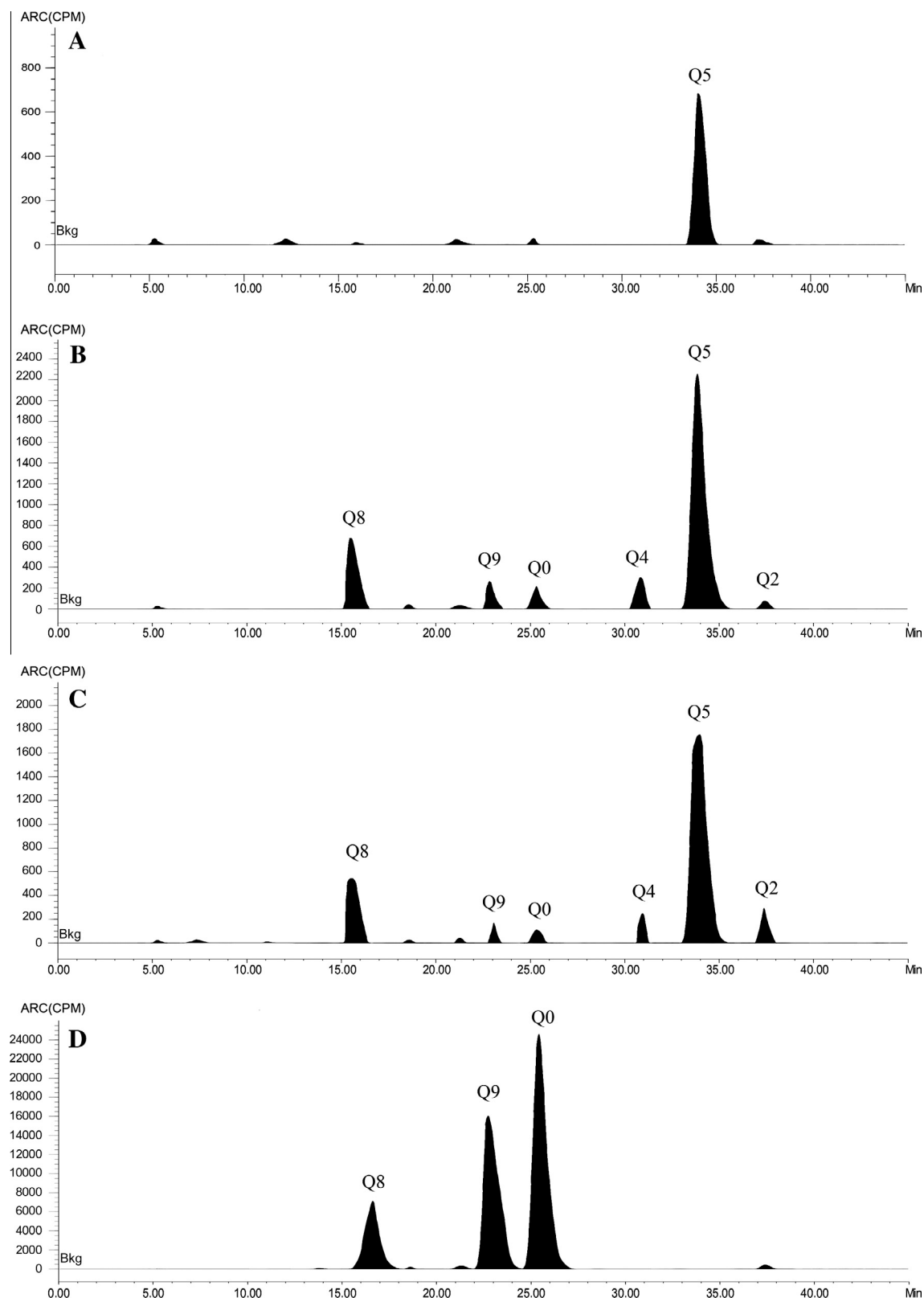


Fig. 3. Metabolite profile of QCT in rats plasma (A, 6 h, radiochromatogram), liver (B, 48 h, radiochromatogram), kidney (C, 48 h, radiochromatogram), urine (D, 0–12 h, radiochromatogram) and feces (E, 0–12 h, radiochromatogram).

Q1, Q2, Q3, Q4, and Q5 in pigs; Q1, Q2, Q3, Q4, and Q7 in broilers; and Q1 and Q2 in carp. The above data indicates that QCT metabolism in rats is different from that in pigs, broilers, and carp.

3.4. Mass spectrometric identification of metabolites

Proposed metabolite structures and supporting spectral data for all matrices are shown in Table 4.

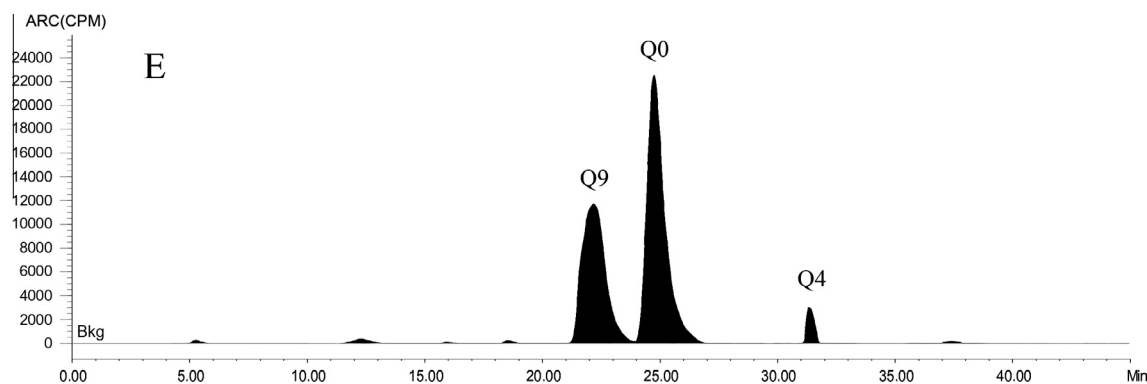


Fig. 3 (continued)

Table 2

Approximate concentration of [^3H]quinocetone and metabolites (μg equivalent per g tissue) in rats and pigs tissues following consecutive 7 days oral administration of [^3H]quinocetone.

Matix	Time (h)	Concentration (µg/kg)						Time (h)	Concentration (µg/kg)						
		Rat							Pig						
		Q0	Q2	Q4	Q5	Q8	Q9		Q0	Q1	Q2	Q3	Q4	Q5	Q6
Liver	6	147 ± 12	280 ± 21	375 ± 29	2562 ± 218	422 ± 34	332 ± 33	6	75 ± 4	118 ± 9	312 ± 23	85 ± 7	83 ± 6	105 ± 7	ND
	48	154 ± 3	100 ± 8	190 ± 9	1007 ± 144	195 ± 18	174 ± 8	24	36 ± 2	68 ± 7	221 ± 19	76 ± 3	29 ± 3	66 ± 5	ND
	120	19 ± 2	31 ± 2	22 ± 3	502 ± 53	36 ± 3	23 ± 2	72	24 ± 3	49 ± 5	201 ± 17	48 ± 2	25 ± 2	64 ± 4	ND
	216	ND ^a	17 ± 1	ND	367 ± 32	ND	ND	168	ND	ND	117 ± 12	ND	ND	ND	ND
Kidney	6	121 ± 4	374 ± 29	292 ± 22	2374 ± 214	500 ± 32	438 ± 38	6	57 ± 2	119 ± 10	264 ± 20	29 ± 3	56 ± 9	82 ± 9	ND
	48	84 ± 7	193 ± 15	181 ± 17	2033 ± 203	210 ± 22	161 ± 15	24	12 ± 2	91 ± 6	169 ± 17	26 ± 3	22 ± 3	36 ± 4	ND
	120	41 ± 3	40 ± 4	77 ± 6	1034 ± 102	82 ± 8	46 ± 5	72	11 ± 2	78 ± 4	138 ± 15	16 ± 2	12 ± 2	21 ± 3	ND
	216	ND	29 ± 1	28 ± 2	515 ± 81	27 ± 1	ND	168	ND	ND	89 ± 10	ND	ND	ND	ND
Muscle	6	10 ± 1	28 ± 2	25 ± 3	211 ± 20	32 ± 3	29 ± 2	6	21 ± 1	28 ± 4	104 ± 12	16 ± 3	25 ± 3	31 ± 3	ND
	48	ND	19 ± 2	21 ± 2	168 ± 16	24 ± 2	19 ± 2	24	ND	16 ± 2	66 ± 7	11 ± 2	14 ± 2	20 ± 2	ND
	120	ND	18 ± 1	16 ± 1	47 ± 4	19 ± 1	ND	72	ND	ND	38 ± 4	ND	ND	ND	ND
Fat	6	19 ± 1	75 ± 7	21 ± 2	438 ± 32	26 ± 2	36 ± 3	6	12 ± 2	27 ± 3	186 ± 22	13 ± 3	27 ± 3	59 ± 7	ND
	48	ND	19 ± 1	14 ± 1	45 ± 4	14 ± 1	14 ± 1	24	ND	22 ± 2	104 ± 12	12 ± 1	12 ± 2	34 ± 4	ND
	120	ND	12 ± 1	11 ± 1	18 ± 1	10 ± 1	ND	72	ND	ND	70 ± 8	ND	ND	ND	ND

^a Not detected. Criteria are no discernible radioactive peak but detected by LC/MS/MS.

The metabolites in plasma, urine, feces, and tissue were qualitatively characterized by LC/MS-IT-TOF. This characterization also included a comparison of the retention times and spectra with synthetic standards. The $[\text{M} + \text{H}]^+$ ion was generally observed in all of the metabolites. Fig. 6 presents the proposed metabolic scheme of QCT in these studied animals.

Because Q0 had the same retention time, MS, and MS² spectrum as QCT, it was identified as the parent drug.

Metabolite Q1 showed a protonated molecular ion at m/z 291, which was 16 Da lower than the protonated molecular ion of QCT. This suggested that it is the N–O group reduction metabolite of QCT. The MS² spectrum identified m/z 274.1090 as the most intense fragment ion, which represents a loss of an OH from m/z 291, and a reduction of the effect of the benzenovinylketo group by the N–O group at position 4. Because of its high intensity, it was identified as 1-desoxyquinocetone because N–O group reduction at position 1 is relatively easier when the electronic effect is considered.

Metabolite Q2 showed a protonated molecular ion at m/z 275, which was 32 Da lower than the protonated molecular ion of QCT. This suggested that it is a dideoxy metabolite of QCT. On the basis of the facts that it had the same fragment ions at m/z 184 and 143 as QCT, Q2 was identified as dideoxyquinocetone.

Metabolite Q3 showed a protonated molecular ion at m/z 293. As show in Table 4, a loss of H₂O lead to the formation of product ions at m/z 275, thus indicating that the reduction occurred on the carbonyl group. The product ion at m/z 258 was formed by the loss

of the OH radical from the product ion at m/z 275, and the product ion at m/z 251 was formed by the loss of C₂H₂O from the protonated molecular ion at m/z 293. This indicated the presence of N–O group at position 1. Thus, Q3 was identified as the carbonyl-reduced metabolite of 4-deoxyquinocetone.

Metabolite Q4 showed a protonated molecular ion at m/z 295, which was 4 Da higher than a protonated molecular ion at m/z 291. This suggested that it is a reduced metabolite of desoxyquinocetone. One explanation is that N–O group reduction at position 1 is enhanced because of the electronic effect, whereas the adjacent methyl group hinders N–O group reduction at position 4. Moreover, the MS² spectrum of the protonated molecule obtained from Q4 showed product ions at m/z 245, 231, and 169. Therefore, metabolite Q4 was identified as both carbonyl- and double bond-reduced metabolites of 1-desoxyquinocetone.

The product ion scan of the protonated molecular ions at m/z 277 of metabolite Q5 indicates a loss of H₂O to form product ions at m/z 259, revealing that the reduction occurred on the carbonyl group. The product ion m/z 259 lost C₆H₆ to form the product ion at m/z 181. Thus, Q5 is identified as the carbonyl-reduced metabolite of dideoxyquinocetone.

Metabolite Q6 showed a protonated molecular ion at m/z 325. Loss of H₂O to form product ions at m/z 307 indicates that the reduction was on the carbonyl group. The product ion at m/z 291 was formed by the loss of two OH radical from the protonated molecular ion at m/z 325. This indicated the presence of N–O group

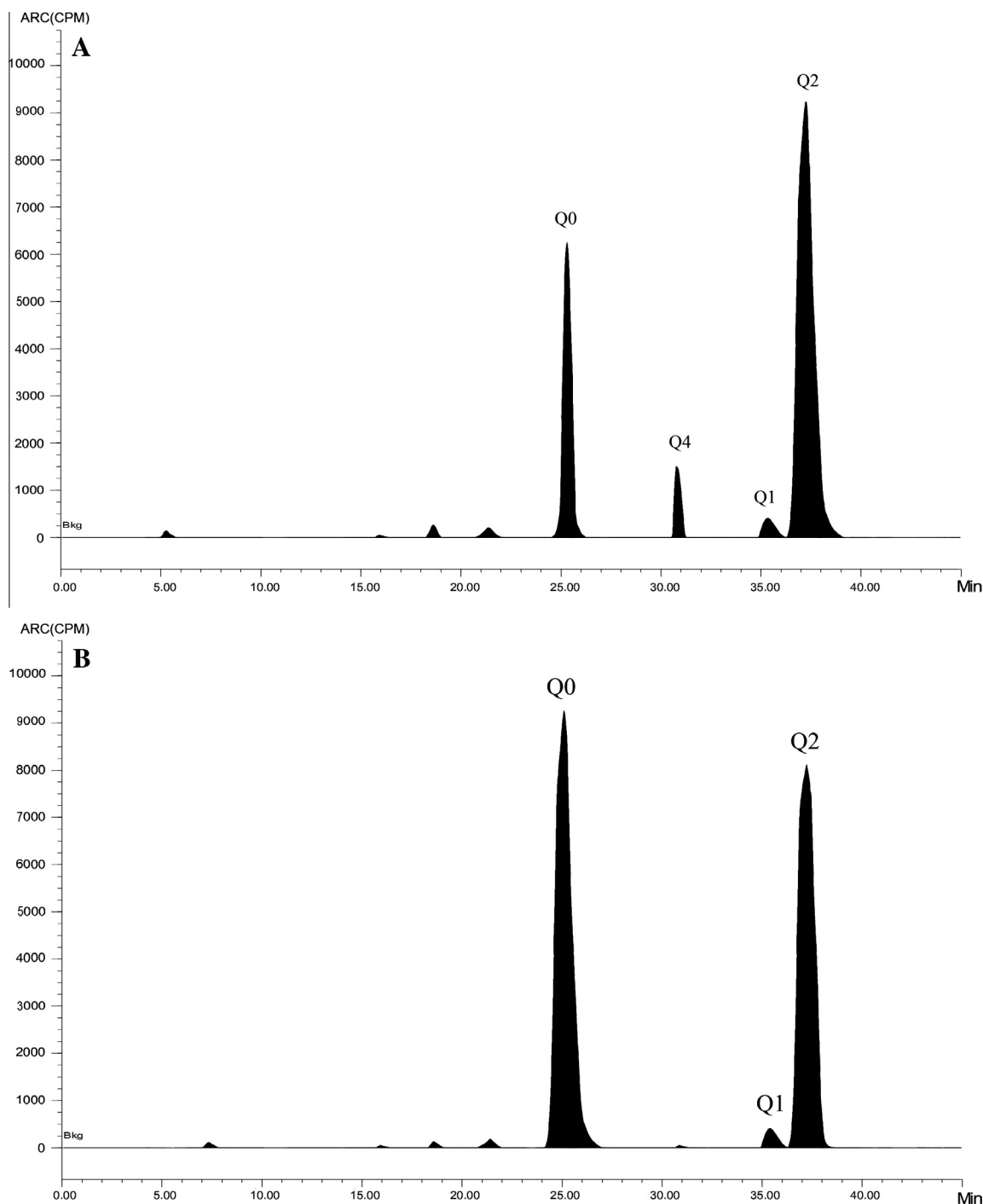


Fig. 4. Metabolite profile of QCT in pigs urine (A, 0–12 h, radiochromatogram) and feces (B, 0–12 h, radiochromatogram).

at positions 1 and 4. The metabolite lost C_6H_6O to form the product ion at m/z 231. This suggested that the position of the hydroxyl group was on the phenyl ring, although the exact position could not be identified.

Metabolite Q7 showed a protonated molecular ion at m/z 309 and formed product ions at m/z 291. This suggested that the reduction occurred on the carbonyl group. The product ion at m/z 274 was formed by the loss of the OH radical from the product ion at m/z 291, followed by the loss of an OH radical to form m/z 257. Therefore, Q7 is identified as the carbonyl-reduced QCT.

Metabolite Q8 showed a protonated molecular ion at m/z 293. As shown in Table 4, the MS^2 spectrum of Q8 showed product ions at

m/z 278 and 265, which were formed by the loss of CH_3 and CO from the precursor ion at m/z 293, respectively, thus indicating that the site of reduction was at the double bond. Thus, Q8 is identified as the double bond-reduced metabolite of 4-deoxyquinocetone.

Metabolite Q9 showed a protonated molecular ion at m/z 323. MS^2 spectra of the protonated molecules obtained from Q9 showed product ions at m/z 278 and 250, which were 16 Da higher than the product ions at m/z 262 and 234 obtained by MS^2 from Q0, respectively. This indicates that it is a hydroxylation metabolite of Q0. Q9 formed the same product ions at m/z 143, 169, 185, and 197 as Q0. This suggested that the position of the hydroxyl group was on the phenyl ring, although the exact position could not be characterized.

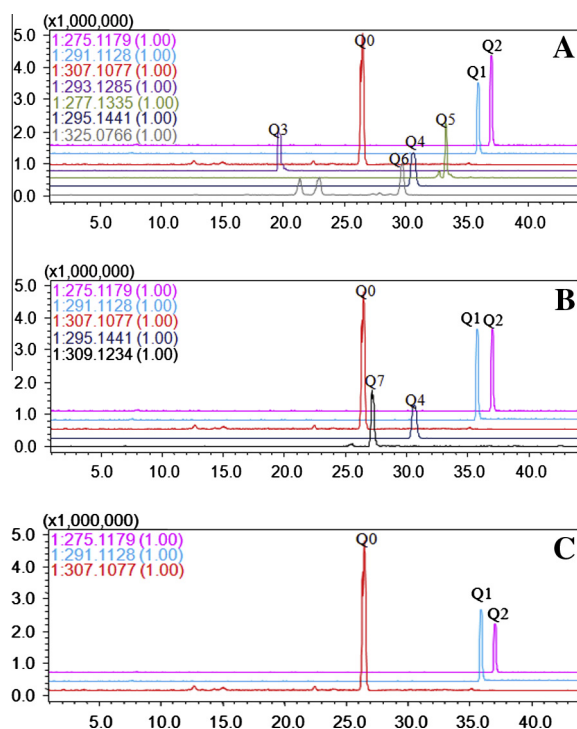


Fig. 5. The accurate extracted ion chromatograph of QCT and its metabolites in pigs bile (A, 6 h), broilers excreta (B, 0–24 h), carp excreta (C, 0–48 h).

Metabolites Q1, Q2, Q3, and Q5 were confirmed by comparison with the standards, and they were eluted at the same retention time and showed the same product ions as the standards.

4. Discussion

QCT excretion was driven by origin and metabolism and was primarily via feces (approximately 70% of the dose). Urine was the secondary route of excretion that cleared approximately 25% of the dose. The recovery of radioactivity was $\geq 98\%$, and for the most part, radioactivity was excreted within 24 h after dose administration in rats and 72 h after dose administration in the

remaining three species. This indicated that QCT absorption in rats after oral administration was rapid compared with that in pigs, broilers, and carp. No evident gender-related difference was observed in the rate of excretion of the drug-related material.

The present study showed that QCT was metabolized extensively, leading to the generation of nine quantitative metabolites. The metabolite profiles in urine suggest that QCT was metabolized via four biotransformation pathways *in vivo*, namely, N–O group reduction, carbonyl group reduction, double bond reduction, and hydroxylation. The N–O group and carbonyl group reduction were the primary pathways, because eight of the characterized metabolites (Q1, Q2, Q3, Q4, Q5, Q6, Q7, and Q8) were formed in these pathways. The N-oxide reduction is catalyzed by several liver enzymes or mediated by the heme groups (Takekawa et al., 2001; Zheng et al., 2011). The results have shown that the metabolites of 1-desoxyquinocetone were larger than those of 4-desoxyquinocetone. Because the electrophilic group next to the 1-N-oxide bond makes the electron density lower than that around the 4-N-oxide bond. Consequently, the less stable 1-N-oxide bond can be more easily reduced. We presume that carbonyl reductases (CBRs) are capable of catalyzing carbonyl group reduction of QCT and its metabolites on the basis of the metabolites found in the present study similar to those of MEQ (Tang et al., 2012). QCT can be catalyzed by CYP1A5 to generate hydrophilic hydroxylation metabolites that are easily excreted, thus preventing drug accumulation (J.N. Yang et al., 2013; Antonovic and Martinez, 2011).

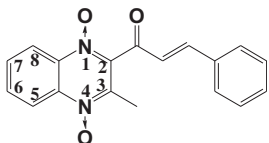
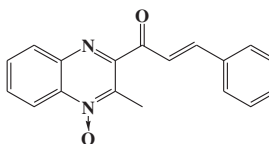
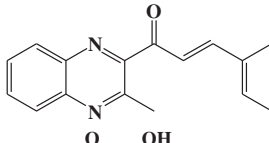
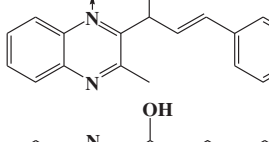
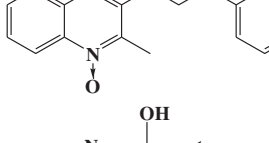
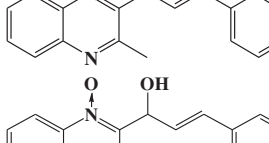
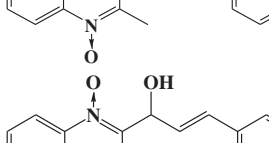
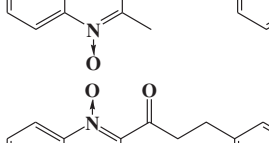
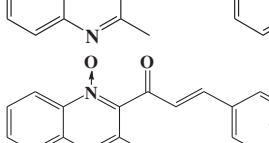
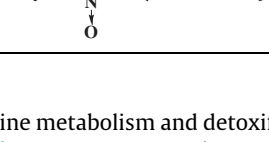
The results of drug distribution studies indicate that after p.o. doses to animals, total radioactivity was generally maximum at 6 h for all the tissues. Radioactivity was detectable in most tissues examined after p.o. doses at 72 h in pigs, broilers, and carp, and at 120 h in rats. This indicated that extensive distribution of QCT or its metabolites in most tissues and slower QCT elimination in rats. Following p.o. administration, the concentrations in the intestinal tract probably represented any unabsorbed drug and the drug secreted in bile. Moreover, the tissue data showed that QCT and/or its metabolites could readily cross the brain barrier and did not associate extensively with erythrocytes. The presence of radioactivity in the reproductive organs shows that these organs would be exposed to the drug and/or its metabolites during reproductive toxicity studies. At every time point, the highest radioactivity levels were found in the liver and kidney, and they were measurable for 7–14 days. This suggested that the liver and kidney function are slow-release depots for the drug. The liver and kidney are vital

Table 3
Approximate concentration of [^3H]quinocetone and metabolites (μg equivalent per g tissue) in broilers and carp tissues following consecutive 7 days oral administration of [^3H]quinocetone.

Matix	Time (h)	Concentration (µg/kg)						Time (h)	Concentration (µg/kg)			
		Broiler							Carp			
		Q0	Q1	Q2	Q3	Q4	Q7		Q0	Q1	Q2	Q4
Liver	6	56 ± 5	186 ± 16	764 ± 59	203 ± 26	136 ± 14	120 ± 14	6	65 ± 4	ND	ND	ND
	24	23 ± 2	105 ± 9	515 ± 31	113 ± 9	36 ± 9	28 ± 8	24	114 ± 12	326 ± 35	217 ± 23	ND
	72	16 ± 2	75 ± 5	432 ± 22	68 ± 8	18 ± 4	19 ± 4	96	ND	99 ± 11	201 ± 21	68 ± 5
	168	ND ^a	ND	158 ± 20	ND	ND	ND	216	ND	ND	25 ± 2	ND
Kidney	6	59 ± 4	158 ± 9	616 ± 58	187 ± 6	76 ± 8	138 ± 8	6	59 ± 2	ND	ND	ND
	24	21 ± 2	112 ± 10	446 ± 25	82 ± 4	57 ± 6	42 ± 5	24	112 ± 12	66 ± 7	91 ± 11	ND
	72	14 ± 1	58 ± 5	345 ± 16	41 ± 3	30 ± 4	18 ± 4	96	ND	58 ± 6	42 ± 6	16 ± 2
	168	ND	ND	132 ± 12	ND	ND	ND	216	ND	ND	19 ± 2	ND
Muscle	6	32 ± 1	59 ± 7	217 ± 26	59 ± 7	31 ± 4	37 ± 8	6	24 ± 2	ND	ND	ND
	24	ND	21 ± 2	97 ± 10	32 ± 3	15 ± 2	20 ± 4	24	ND	12 ± 2	ND	ND
	72	ND	ND	89 ± 8	ND	ND	ND					
Fat(Skin)	6	33 ± 1	35 ± 5	249 ± 26	71 ± 6	14 ± 2	24 ± 3	6	72 ± 8	ND	ND	ND
	24	ND	22 ± 4	131 ± 13	26 ± 3	11 ± 1	10 ± 1					
	72	ND	ND	74 ± 5	ND	ND	ND					

^a Not detected. Criteria are no discernible radioactive peak but detected by LC/MS/MS.

Table 4Relevant metabolites of [³H]quinoxetone in animals italicized metabolites have been confirmed with comparison with standards.

Compound	[M + H] ⁺ (Da)	Proposed structure	Major product ions
Q0	307		290, 273, 262, 245, 234, 231, 217, 214, 197, 184, 171, 169, 160, 143, 131
Q1	291		274, 246, 231, 187, 183, 159, 131
Q2	275		247, 232, 169, 145, 143, 119
Q3	293		275, 258
Q4	295		277, 260, 245, 232, 169
Q5	277		259, 181, 131
Q6	325		307, 291, 231, 143
Q7	309		291, 274, 257
Q8	293		278, 265, 251, 187, 146, 145
Q9	323		278, 250, 197, 185, 169, 143

target organs responsible for quinoxaline metabolism and detoxification (Fang et al., 2006; X. Wang et al., 2011; WHO, 1991). Recent investigations have showed that QCT had selective toxicity to the liver and kidney, could accelerate bile duct hyperplasia and lead to renal dysfunction by the stimulation of DNA damage and oxidative stress at a high dose (Wang et al., 2010; Yu et al., 2013).

The activities of certain N-oxide compounds that function as important pharmacological or toxicological agents were presumed to depend on the presence of their N-oxide groups (Nunoshiba and

Nishioka, 1989). N-oxide reduction is driven by single-electron reductases (Liu et al., 2010b). Single-electron reduction of quinoxaline-N,N-dioxides leads to DNA damage by radical intermediate production (Ganley et al., 2001). Therefore, QCT toxicities may be mainly attributed to N-oxide reduction that leads to the production of some radical intermediates. ROS plays important roles in QdNO-induced pathological processes (Chowdhury et al., 2004; Azqueta et al., 2007; Badham and Winn, 2010; Huang et al., 2009, 2010). Quinoxaline-2-carboxylic acid (QCA), a completely

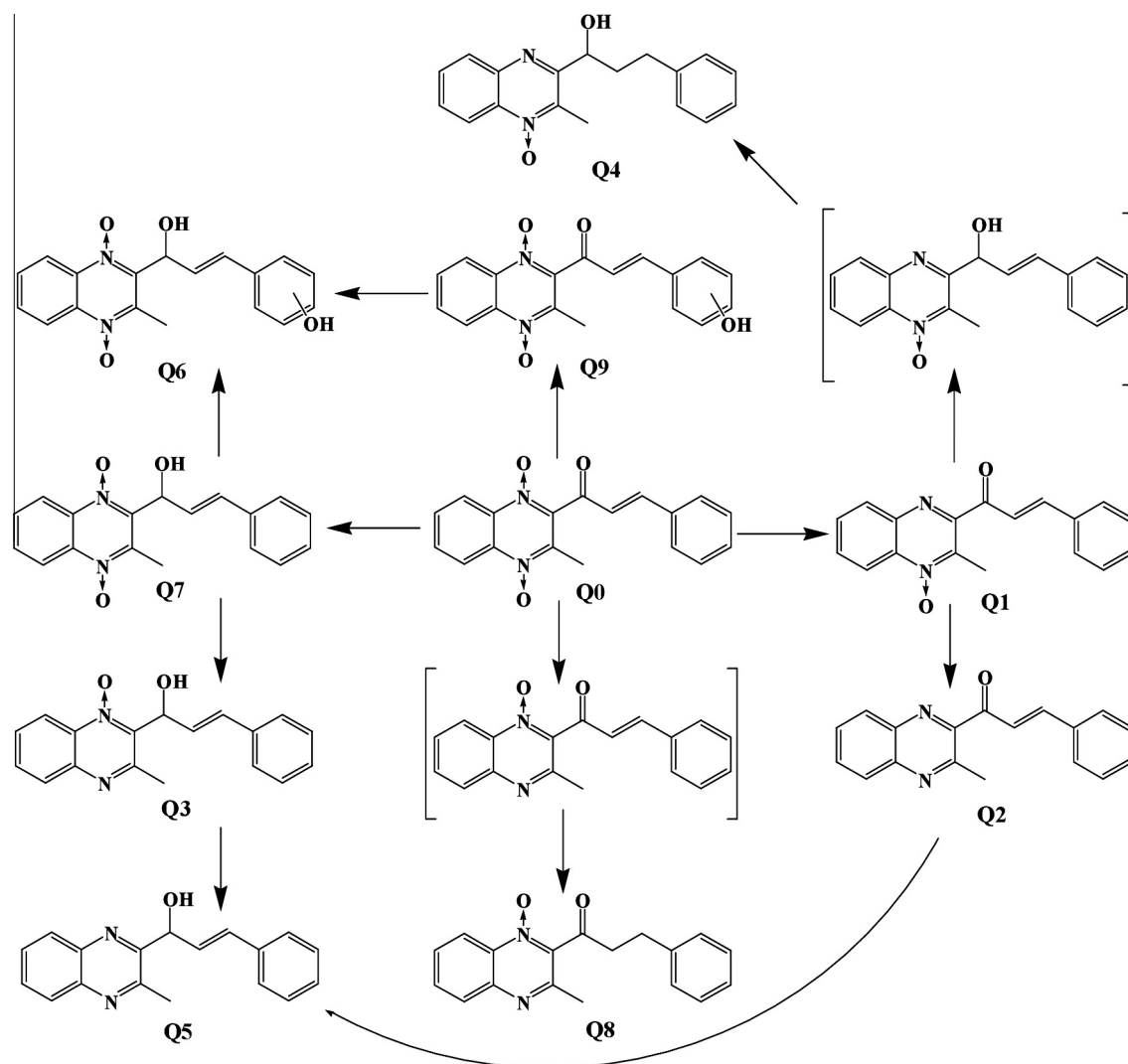


Fig. 6. Proposed metabolic scheme of QCT.

reduced derivative of CBX, did not generate significant amounts of ROS and showed relatively lower toxicity than its parent molecules (Huang et al., 2010). Therefore, two bisdesoxyquinocetone metabolites (Q2 and Q5) were expected to be less toxic than four other desoxyquinocetone metabolites (Q1, Q3, Q4, and Q8), and Q0 could be the most toxic compound depending on the presence of two N-oxide groups.

In rat tissues, Q5 and Q8 were the main metabolites, Q8 was believed to be one of the main toxic metabolites because of its relatively greater peak area over the other desoxyquinocetone and the damage resulted from progressive N-O group reduction. However, the results are much different from those obtained *in vitro* (Liu et al., 2010a). The results of this *in vitro* study demonstrated that Q1 and Q3 were the main metabolites and the relative percentage of Q8 was very low when QCT was incubated with the liver microsomes of rats. The results of our study showed that the pathway of QCT metabolism *in vivo* was much different from that reported *in vitro*. In pigs, broilers, and carp tissues, Q1 was believed to be the main toxic metabolite. It indicated that QCT metabolism in rats is different from that in pigs, broilers, and carp, probably due to the difference in the enzymatic mechanism and the expression levels of the relevant enzymes in the liver. The tissue depletion of QCT and its metabolites needs further investigation. Of note, Q1 and Q8 concentrations in both the liver and kidney

samples were similar. The potential mechanism may be that much more desoxyquinocetone was produced in the liver, such as Q1 and Q8, resulting in liver damage, while the excessive amounts of Q1 and Q8 were transported to other organs such as the kidney. The results directly testified for the relationship between the metabolism of QCT and its potential toxicity *in vivo*. The data of the present study speculate that the liver and kidney are exposed to significant amounts of QCT, which can lead to the formation of several N-O reduction metabolites and then cause bile duct hyperplasia or nephrotoxicity by inducing ROS generation. However, the exact mechanism needs to be determined.

In summary, QCT is extensively metabolized in rats, pigs, broilers, and carp, primarily involving N-O group reduction, carbonyl group reduction, and hydroxylation pathways. Fecal excretion was the major route of elimination of the dosed radioactivity in the four species studied, whereas renal elimination was the second route. All available data show that liver and kidney are major organs involved in QCT clearance and toxicity in the body. Several differences were observed in the various species. The major metabolites of QCT were Q2, Q4, Q5, Q8, and Q9 in rats; Q1, Q2, Q3, Q4, and Q5 in pigs; Q1, Q2, Q3, Q4, and Q7 in broilers; and Q1 and Q2 in carp. The metabolism, disposition, and excretion studies of QCT offer a good model for the evaluation of the toxicology and development of the practical applications of experimental

veterinary drugs, and thus provide a basic foundation for the formulation of safety controls for products obtained from animals.

Conflict of Interest

The authors declare that there are no conflicts of interest.

Transparency Document

The [Transparency document](#) associated with this article can be found in the online version.

Acknowledgements

This work was supported by Grants from Special Fund for Agro-scientific Research in the Public Interest (No. 201203040), National Natural Science Foundation of China (No. 31272614), National Basic Research Program of China (No. 2009CB118800), Recommend international advanced agricultural science and technology plan (No. 2011-G4) and the Project of Excellence FIM UHK.

References

- Antonovic, L., Martinez, M., 2011. Role of the cytochrome P450 enzyme system in veterinary pharmacokinetics: where are we now? where are we going? *Future Med. Chem.* 3, 855–879.
- AVMA, 2001. Panel on Euthanasia 2000 Report of the AVMA panel on euthanasia. *J. Am. Veter. Med. Assoc.* 218, 669.
- Azqueta, A., Arbillaga, L., Pachon, G., Cascante, M., Creppy, E.E., Lopez de Cerain, A., 2007. A quinoxaline 1,4-di-N-oxide derivative induces DNA oxidative damage not attenuated by vitamin C and E treatment. *Chem. Biol. Interact.* 168, 95–105.
- Badham, H.J., Winn, L.M., 2010. In utero exposure to benzene disrupts fetal hematopoietic progenitor cell growth via reactive oxygen species. *Toxicol. Sci.* 113, 207–215.
- Beutin, L., Preller, E., Kowalski, B., 1981. Mutagenicity of quinoxin, its metabolites, and two substituted quinoxaline-di-N-oxides. *Antimicrob. Agents Chemother.* 20, 336–343.
- Chen, Q., Tang, S.S., Jin, X., Zou, J.J., Chen, K.P., Zhang, T., Xiao, X.L., 2009. Investigation of the genotoxicity of quinocetone, carbadox and olaquinox in vitro using Vero cells. *Food Chem. Toxicol.* 47, 328–334.
- Chowdhury, G., Kotandeniya, D., Daniels, J.S., Barnes, C.L., Gates, K.S., 2004. Enzyme-activated, hypoxia-selective DNA damage by 3-amino-2-quinoxalinecarbonitrile 1,4-di-N-oxide. *Chem. Res. Toxicol.* 17, 1399–1405.
- Fang, G., He, Q., Zhou, S., Wang, D., Zhang, Y., Yuan, Z., 2006. Subchronic oral toxicity study with cyadox in Wistar rats. *Food Chem. Toxicol.* 44, 36–41.
- FAO/WHO, 1990. Joint Expert Committee on Food Additives: evaluation of certain veterinary drug residues in food. 799, 45–54.
- FAO/WHO, 1995. Joint Expert Committee on Food Additives: evaluation of certain veterinary drug residues in food. 851, 19–22.
- Ganley, B., Chowdhury, G., Bhansali, J., Scott Daniels, J., Gates, K.S., 2001. Redoxactivated, hypoxia-selective DNA cleavage by quinoxaline 1,4-di-N-oxide. *Bioorg. Med. Chem.* 9, 2395–2401.
- Hu, G.M., Huang, L.L., Yuan, Z.H., 2008. Pharmacokinetics and residue depletion of quinocetone in carp. *Huazhong Agric. Univ.*
- Huang, X.J., Zhang, H.X., Wang, X., Huang, L.L., Zhang, L.Y., Yan, C.X., Liu, Y., Yuan, Z.H., 2010. ROS mediated cytotoxicity of porcine adrenocortical cells induced by QdNOs derivatives in vitro. *Chem. Biol. Interact.* 185, 227–234.
- Huang, X.J., Ihsan, A., Wang, X., Dai, M.H., Wang, Y.L., Su, S.J., Xue, X.J., Yuan, Z.H., 2009. Long-term dose-dependent response of Mequinox on aldosterone, corticosterone and five steroidogenic enzyme mRNAs in the adrenal of male rats. *Toxicol. Lett.* 191, 167–173.
- Ihsan, A., Wang, X., Zhang, W., Tu, H.G., Wang, Y.L., Huang, L.L., Iqbal, Z., Cheng, G.Y., Pan, Y.H., Liu, Z.L., Tan, Z.Q., Zhang, Y.Y., Yuan, Z.H., 2013. Genotoxicity of quinocetone, cyadox and olaquinox in vitro and in vivo. *Food Chem. Toxicol.* 59, 207–214.
- Li, J.Y., Li, J.S., Zhao, R.C., Miao, X.L., Zhang, J.Y., Zhou, X.Z., 2008. Study on residues of quinocetone in edible chicken tissues. *Prog. Veter. Med.* 29 (4), 34–37.
- Liu, Z.Y., Huang, L.L., Chen, D.M., Dai, M.H., Tao, Y.F., Wang, Y.L., Yuan, Z.H., 2010a. Application of electrospray ionization hybrid ion trap/time-of-flight mass spectrometry in the rapid characterization of quinocetone metabolites formed in vitro. *Anal. Bioanal. Chem.* 396 (3), 1259–1271.
- Liu, Z.Y., Huang, L.L., Chen, D.M., Dai, M.H., Tao, Y.F., Yuan, Z.H., 2010b. The metabolism and N-oxide reduction of olaquinoxin liver preparations of rats, pigs and chicken. *Toxicol. Lett.* 195, 51–59.
- Nunoshiba, T., Nishioka, H., 1989. Genotoxicity of quinoxaline 1,4-dioxide derivatives in *Escherichia coli* and *Salmonella typhimurium*. *Mutat. Res.* 217, 203–209.
- Takekawa, K., Sugihara, K., Kitamura, S., Ohta, S., 2001. Enzymatic and non-enzymatic reduction of brucine N-oxide by aldehyde oxidase and catalase. *Xenobiotica* 31, 769–782.
- Tang, X.Q., Mu, P.Q., Wu, J., Jiang, J., Zhang, C.H., Zheng, M., Deng, Y.Q., 2012. Carbonyl reduction of requinox by chicken and porcine cytosol and cloned CBR1. *Drug Metab. Dispos.* 40 (4), 788–795.
- VICH GL 46, 2010. Studies to Evaluate the Metabolism and Residue Kinetics of Veterinary Drugs in Food-producing Animals: Metabolism Study to Determine the Quantity and Identify the Nature of Residues (MRK).
- Wang, D., Luo, X., Zhong, Y., Yang, W., Xu, M.J., Liu, Y., Meng, J., Yao, P., Yan, H., Liu, L.G., 2012. Pu-erh black tea extract supplementation attenuates the oxidative DNA damage and oxidative stress in Sprague–Dawley rats with renal dysfunction induced by subchronic 3-methyl-2-quinoxalin benzenevinylketo-1,4-dioxide exposure. *Food Chem. Toxicol.* 50, 147–154.
- Wang, D., Zhong, Y., Luo, X., Wu, S., Xiao, R., Bao, W., Yang, W., Yan, H., Yao, P., Liu, L.G., 2011. Pu-erh black tea supplementation decreases quinocetone-induced ROS generation and oxidative DNA damage in Balb/c mice. *Food Chem. Toxicol.* 49, 477–484.
- Wang, X., Zhang, W., Wang, Y.L., Ihsan, A., Dai, M.H., Huang, L.L., Chen, D.M., Tao, Y.F., Peng, D.P., Liu, Z.L., Yuan, Z.H., 2012. Two generation reproduction and teratogenicity studies of feeding quinocetone fed to Wistar rats. *Food Chem. Toxicol.* 50 (5), 1600–1609.
- Wang, X., Huang, X.J., Ihsan, A., Liu, Z.Y., Huang, L.L., Zhang, H.H., Zhang, H.F., Zhou, W., Liu, Q., Xue, X.J., Yuan, Z.H., 2011. Metabolites and JAK/STAT pathway were involved in the liver and spleen damage in male Wistar rats fed with mequinox. *Toxicology* 280 (3), 126–134.
- Wang, X., Zhang, W., Wang, Y.L., Peng, D.P., Ihsan, A., Huang, X.J., Huang, L.L., Liu, Z.L., Dai, M.H., Zhou, W., Yuan, Z.H., 2010. Acute and sub-chronic oral toxicological evaluations of quinocetone in Wistar rats. *Regul. Toxicol. Pharm.* 58, 421–427.
- WHO (World Health Organization), 1991. Toxicological evaluation of certain veterinary drug residues in food. Carbadox. WHO Food Additives Series, No. 27, no. 700 on INCHEM.
- Wu, H.X., Yang, C.Y., Wang, Z.H., Shen, J.Z., Zhang, S.X., Feng, P.S., Li, L.X., Cheng, L.L., 2012. Metabolism profile of quinocetone in swine by ultra-performance liquid chromatography quadrupole time-of-flight mass spectrometry. *Eur. J. Drug Metab. Ph.* 37 (2), 141–154.
- Yang, J.N., Liu, Z.Y., Li, M., Qiu, X.H., 2013. Hydroxylation of quinocetone and carbadox is mediated by CYP1As in the chicken (*Gallus gallus*). *Comp. Biochem. Phys. C* 158, 84–90.
- Yang, W., Fu, J., Xiao, X., Yan, H., Bao, W., Wang, D., Hao, L.P., Nussler, A.K., Yao, P., Liu, L.G., 2013. Quinocetone triggers oxidative stress and induces cytotoxicity and genotoxicity in human peripheral lymphocytes of both genders. *J. Sci. Food Agric.* 93, 1317–1325.
- Yu, M., Xu, M.J., Liu, Y., Yang, W., Rong, Y., Yao, P., Yan, H., Wang, D., Liu, L.G., 2013. Nrf2/ARE is the potential pathway to protect Sprague–Dawley rats against oxidative stress induced by quinocetone. *Regul. Toxicol. Pharm.* 66, 279–285.
- Zhang, K., Ban, M.M., Zhao, Z.Z., Zheng, H.H., Wang, X., Wang, M., Fei, C.Z., Xue, F.Q., 2012. Cytotoxicity and genotoxicity of 1,4-bisdesoxyquinocetone, 3-methyl-quinoxaline-2-carboxylic acid (MQCA) in human hepatocytes. *Res. Veter. Sci.* 93, 1393–1401.
- Zheng, M., Jiang, J., Wang, J.P., Tang, X.Q., Ouyang, M., Deng, Y.Q., 2011. The mechanism of enzymatic and non-enzymatic N-oxide reductive metabolism of cyadox in pig liver. *Xenobiotica* 41, 964–971.
- Zhong, J.L., Wang, L., Zhao, N., Yu, H.M., Jia, H.Q., Lu, X.X., Wu, Z.Y., Ding, H.Z., 2012. Study on residue depletion of quinocetone and its major metabolites in swine. *J. South China Agric. Univ.* 33 (2), 248–252.